

Dynamic Wind Effects on Buildings with 3D Coupled Modes: Application of High Frequency Force Balance Measurements

Xinzhong Chen¹ and Ahsan Kareem²

Abstract: Contemporary high-rise buildings with complex geometric profiles and three-dimensional (3D) coupled mode shapes often complicate the use of high frequency force balance (HFFB) technique customarily used in wind tunnel testing for uncoupled buildings. In this study, a comprehensive framework for the coupled building response analysis and the modeling of the associated equivalent static wind loads using the HFFB measurement is presented. This includes modeling of building structural systems whose mass centers at different floors may not be located on a single vertical axis. The building response is separated into the mean, background, and resonant components, which are quantified by modal analysis involving three fundamental modes in two translational and torsional directions. The equivalent static wind load is described in terms of the modal inertial loads. The proposed framework takes into account the cross correlation of wind loads acting in different primary directions and the intermodal coupling of modal responses with closely spaced frequencies. Wind load combination is revisited in the context of modeling of the equivalent static wind loads. A representative tall building with 3D coupled modes and closely spaced frequencies is utilized to demonstrate the proposed framework and to highlight the significance of cross correlation of wind loads and the intermodal coupling of modal responses on the accurate prediction of coupled building response. Additionally, delineation of the proper role of the correlation between integrated loads, modal response, and respective building response components in the evaluation of wind effects on coupled buildings is underscored.

DOI: 10.1061/(ASCE)0733-9399(2005)131:11(1115)

CE Database subject headings: Wind loads; Motion; Damping; Structural dynamics; Buildings, high-rise.

Introduction

The wind-induced building response can be generally separated into the mean (static), background (quasistatic) and resonant components. Predictions of the mean and background response components using the static and quasistatic analyses involving influence functions result in more accurate estimates than the modal analysis based on only three fundamental modes in translational and torsional directions. Whereas, the modal analysis offers sufficiently accurate prediction of the resonant response component (e.g., Chen and Kareem 2005a). Wind loads may be derived through multiple point synchronous scanning of pressures or by measured forces on the model mounted on a high frequency force balance (HFFB). The simultaneously monitored pressure database offers great flexibility in deriving mode generalized loads for buildings with mode shapes that depart from linear or exhibit coupling. However, for tall buildings with dominant resonant response, both the mean and background response components can

be approximately quantified by the modal analysis when only integrated wind loads through HFFB measurements are available.

The HFFB measurements have been widely recognized for conveniently quantifying generalized wind forces on tall buildings with uncoupled mode shapes (e.g., Kareem and Cermak 1979; Tschanz and Davenport 1983; Reinhold and Kareem 1986; Boggs and Peterka 1989). The generalized forces are then utilized for estimating building response with given structural characteristics. The HFFB technique generally requires mode shape corrections which are either based on empirical corrections, or analytical formulations derived on the basis of assumed wind loading models (e.g., Vickery et al. 1985; Boggs and Peterka 1989; Xu and Kwok 1993; Zhou et al. 2002; Holmes et al. 2003; Chen and Kareem 2004a).

The HFFB measurements have also been utilized for identifying spatiotemporally varying dynamic wind loads on buildings (Ohkuma et al. 1995; Yip and Flay 1995; Solari et al. 1998; Xie and Irwin 1998). In these studies, analytical wind loading models with unknown parameters are assumed in the frequency domain in terms of their spectral descriptions (Ohkuma et al. 1995; Yip and Flay 1995; Solari et al. 1998), or in the time domain in terms of their spatial distributions (Xie and Irwin 1998). These unknown parameters are then identified using the base force measurements. Once the dynamic wind loads are determined, any response component of interest can be subsequently analyzed using actual building dynamics without introducing any mode shape correction procedure. It has been pointed out that, akin to the traditional HFFB technique, the accuracy of these identification schemes depends on the efficacy of the assumed wind loading models (Chen and Kareem 2005b).

Buildings with complex geometric shapes or structural systems with noncoincident centers of mass and resistance, or both,

¹Assistant Professor, Wind Science and Engineering Research Center, Dept. of Civil Engineering, Texas Tech Univ., Lubbock, TX 79409 (corresponding author). E-mail: xinzhong.chen@ttu.edu

²Robert M. Moran Professor, NatHaz Modeling Laboratory, Dept. of Civil Engineering and Geological Sciences, Univ. of Notre Dame, Notre Dame, IN 46556. E-mail: kareem@nd.edu

Note. Associate Editor: Nicos Makris. Discussion open until April 1, 2006. Separate discussions must be submitted for individual papers. To extend the closing date by one month, a written request must be filed with the ASCE Managing Editor. The manuscript for this paper was submitted for review and possible publication on June 17, 2004; approved on December 28, 2004. This paper is part of the *Journal of Engineering Mechanics*, Vol. 131, No. 11, November 1, 2005. ©ASCE, ISSN 0733-9399/2005/11-1115-1125/\$25.00.

may undergo three dimensional (3D) coupled motions when exposed to spatiotemporally varying dynamic wind loads. The prediction of coupled building response requires use of analysis frameworks that take into account the cross correlation of wind loads acting in different primary directions and the intermodal coupling of modal responses (e.g., Kareem 1985; Tallin and Ellingwood 1985; Shimada et al. 1990; Islam et al. 1992; Flay et al. 1999; Chen and Kareem 2005a). The HFFB measurements can be readily incorporated into the analysis frameworks when the mass centers of all floors lie on a single vertical axis and the mode shapes are assumed to be linear functions over the building height (Kareem 1985; Tallin and Ellingwood 1985; Shimada et al. 1990; Islam et al. 1992). The application of HFFB measurements to buildings with general 3D coupled modes have been studied in Irwin and Xie (1993), Yip and Flay (1995), Holmes et al. (2003), and Chen and Kareem (2004a).

The intermodal coupling is often considered by utilizing the complete quadratic combination (CQC) rule to combine the modal responses for estimating total dynamic response. The modal correlation coefficient between two adjacent modes is often estimated using the closed-form formulation given in Der Kiureghian (1980) for the analysis of wind load effects on buildings and other structures (e.g., Xie et al. 2003). It has been emphasized in Chen and Kareem (2005a) that this formulation is only valid when the generalized forces are fully correlated as in the case of buildings with a single earthquake excitation. The modal correlation coefficient depends not only on the frequencies and damping ratios, but also on the correlation/coherence of the generalized forces. Utilization of the formulation in Der Kiureghian (1980) will overestimate the modal correlation associated with multiple excitations of partially correlated wind loads.

The equivalent static wind load (ESWL) representation of the dynamic wind loads has been widely adopted in building codes and standards. It also serves as a useful tool to provide simplified representation of dynamic wind loads derived from wind tunnel testing for design applications. The ESWL given by the gust response factor (GRF) approach, introduced by Davenport (1967) for the alongwind loading and adopted worldwide in building codes and standards, results in a load distribution similar to the mean wind load. A number of studies have suggested physically more meaningful load descriptions featuring dynamic wind load characteristics and modal inertial loads (e.g., Davenport 1985; Boggs and Peterka 1989; Kasperski 1992; Zhou and Kareem 2001; Chen and Kareem 2001, 2004b, 2005a; Holmes 2002; Kareem and Zhou 2003; Repetto and Solari 2004).

Modeling of the ESWL for coupled building response, like the ESWL for combined wind load effects of uncoupled buildings, warrants a discussion regarding the combination of wind loads acting in different primary directions. The alongwind and acrosswind load combinations for uncoupled buildings have been discussed by Melbourne (1975), Vickery and Basu (1984), and Solari and Pagnini (1999). The ASCE 7-02 standard (ASCE 2000) and the National Building Code of Canada (NBCC 1995) suggest a load combination factor of 0.75 to reflect the combined action of any two wind load components. The latest version of Japanese building code, *AIJ-RLB-2004* (Tamura et al. 2003a), addresses the combination of alongwind, acrosswind, and torsional loads based on the studies by Asami (2000) and Tamura et al. (2003b).

This paper focuses on the HFFB technique for buildings with 3D coupled modes. A response analysis framework is proposed for buildings with mass centers at different floors that may not align on a single vertical axis. Formulations for the estimation of the generalized forces with modal shape corrections, analysis of

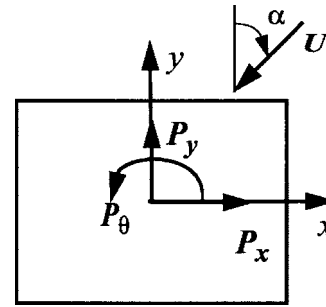


Fig. 1. Coordinate system and wind orientation

any dynamic response of interest, and modeling of ESWL for a given peak response are presented. The wind load combination is revisited in the context of modeling of ESWLs. A representative tall building with 3D coupled modes and closely spaced mode frequencies is utilized to demonstrate the proposed framework, and to highlight the significance of cross correlation of wind loads and the intermodal coupling of modal responses on the building response. The distinct role of the correlation between integrated loads, modal response, and respective building response components is highlighted.

General Formulation

Generalized Wind Forces

A wind-excited tall building at a given wind speed and direction is considered for analysis. A Cartesian coordinate system with two orthogonal translational axes x and y and vertical axis z with the origin at the ground is used for describing the building system (Fig. 1). The i th floor of the building at the elevation z_i above the ground has a lumped mass m_i , and a polar moment of inertia I_i about the mass center of the floor ($i=1, 2, \dots, N$; N =total floor number). The mass center of the i th floor is located at the point with the coordinates $(x, y, z) = (e_{ix}, e_{iy}, z_i)$. The mass centers at different floors may not be located on a single vertical axis.

The HFFB measurements, using a scaled building model under simulated wind field, provide direct estimates of the integrated wind loads in terms of the base bending moments along the axes x and y , and base torque about the axis z , i.e., $M_s(t)$ ($s=x, y, \theta$). The HFFB is attached to the building model at the coordinates $(x, y, z) = (0, 0, 0)$. These quantities for both the scaled building model and the prototype are related by the following similarity relationship:

$$M_s(t) = M_{sm}(t_m) / (\lambda_\rho \lambda_L^3 \lambda_U^2) \quad (s = x, y, \theta) \quad (1)$$

$$f S_{M_{sl}}(f) = f_m S_{M_{slm}}(f_m) / (\lambda_\rho \lambda_L^3 \lambda_U^2) \quad (s, l = x, y, \theta) \quad (2)$$

$$t_m = t \lambda_U / \lambda_L \quad (3)$$

$$f_m = f \lambda_U / \lambda_L$$

where $\lambda_\rho = \rho_m / \rho$, $\lambda_L = B_m / B$, and $\lambda_U = U_m / U$ represent air density, length, and wind speed scaling parameters; B =representative width of the building; U =reference wind speed; t and f =time and frequency; $S_{M_{ss}}(f)$ and $S_{M_{sl}}(f)$ =power spectral density (PSD) of $M_s(t)$ and the cross power spectral density (XPSD) between $M_s(t)$ and $M_l(t)$; and subscript m denotes the quantities for the scaled building model.

To establish the relationships between the generalized forces and the base force measurements, the wind load acting on the i th floor in s direction at the location with the coordinate $(x, y, z) = (0, 0, z_i)$ is defined to have a mean (static) and a fluctuating (dynamic) component, \bar{P}_{is} and $P_{is}(t)$, respectively. Consequently, the mean and fluctuating base bending moments and torque can be expressed as

$$\bar{M}_s = \sum_{i=1}^N z_i^{\beta'_s} \bar{P}_{is} \quad (4)$$

$$M_s(t) = \sum_{i=1}^N z_i^{\beta'_s} P_{is}(t)$$

where $\beta'_s = 1$ when $s = x$ or y ; and $\beta'_s = 0$ when $s = \theta$.

On the other hand, the corresponding mean and fluctuating components of the j th generalized force, \bar{Q}_j and $Q_j(t)$ ($j=1, 2, 3$), are given by

$$\bar{Q}_j = \sum_{i=1}^N (\Theta_{ijx} \bar{P}_{ix} + \Theta_{ijy} \bar{P}_{iy} + \Theta_{ij\theta} \bar{P}_{i\theta}) \quad (5)$$

$$Q_j(t) = \sum_{i=1}^N (\Theta_{ijx} P_{ix}(t) + \Theta_{ijy} P_{iy}(t) + \Theta_{ij\theta} P_{i\theta}(t)) \quad (6)$$

where Θ_{ijx} , Θ_{ijy} , and $\Theta_{ij\theta} = j$ th 3D mode shape components in terms of the building motions at the point on the i th floor with the coordinate $(x, y, z) = (0, 0, z_i)$. These mode shapes are derived from the structural model of the building which may encompass eccentricities in the centers of mass and stiffness at each floor.

The mean and XPSD matrix of the generalized forces, $\{\bar{Q}\} = \{\bar{Q}_j\}$ and $[S_Q(f)] = [S_{Q_{jk}}(f)]$, can be expressed in terms of those of the base bending moments and torque, $\{\bar{M}\} = \{\bar{M}_s\}$ and $[S_M(f)] = [S_{M_{st}}(f)]$, and the adequately defined mode shape corrections, $[\bar{\eta}] = [\bar{\eta}_{js}]$ and $[\eta(f)] = [\eta_{js}(f)]$

$$\{\bar{Q}\} = [\bar{\eta}]\{\bar{M}\} \quad (7)$$

$$[S_Q(f)] = [\eta(f)][S_M(f)][\eta(f)]^T \quad (8)$$

$$\bar{\eta}_{js} = \frac{\sum_{i=1}^N \Theta_{ijs} \bar{P}_{is}}{\sum_{i=1}^N z_i^{\beta'_s} \bar{P}_{is}} \quad (9)$$

$$\eta_{js}^2(f) = \frac{\sum_{i=1}^N \sum_{k=1}^N \Theta_{ijs} \Theta_{kjs} S_{P_{iks}}(f)}{\sum_{i=1}^N \sum_{k=1}^N z_i^{\beta'_s} z_k^{\beta'_s} S_{P_{iks}}(f)} \quad (10)$$

where $S_{Q_{jj}}(f)$ and $S_{Q_{jk}}(f) = \text{PSD}$ of $Q_j(t)$ and the XPSD between $Q_j(t)$ and $Q_k(t)$ ($j, k=1, 2, 3$); $S_{P_{iks}}(f) = \text{XPSD}$ between $P_{is}(t)$ and $P_{ks}(t)$; and superscript T denotes the matrix transpose operator.

It is obvious that for buildings whose 3D mode shapes vary linearly in translational directions and uniformly in torsion over the building height, the generalized forces can then be accurately quantified from the base bending moments and torque. Otherwise, the mode shape corrections have to be estimated using empirical

or analytical formulations derived based on presumed wind loading models (Vickery et al. 1985; Boggs and Peterka 1989; Xu and Kwok 1993; Zhou et al. 2002; Holmes et al. 2003; Chen and Kareem 2004b).

For example, when the building mode shape and wind loading are expressed as

$$\Theta_{ijs} = \Theta_{js0} \left(\frac{z_i}{H} \right)^{\beta_s} \quad (11)$$

$$\bar{P}_{is} = \bar{P}_{s0} \left(\frac{z_i}{H} \right)^{\alpha_{s0}} \quad (12)$$

$$S_{P_{iks}}(f) = S_{P_{s0}}(f) \left(\frac{z_i}{H} \right)^{\alpha_s} \left(\frac{z_k}{H} \right)^{\alpha_s} \exp \left(- \frac{k_{zs} f |z_i - z_k|}{U_H} \right) \quad (13)$$

the mode shape corrections are then given by (Chen and Kareem 2004b)

$$\bar{\eta}_{js} = \left(\frac{\Theta_{js0}}{H^{\beta'_s}} \right) \left(\frac{1 + \alpha_s + \beta'_s}{1 + \alpha_s + \beta_s} \right) \quad (14)$$

$$\eta_{js}(f) = \left(\frac{\Theta_{js0}}{H^{\beta'_s}} \right) \left(\frac{1 + \alpha_s + \beta'_s}{1 + \alpha_s + \beta_s} \right) \sqrt{\frac{1 + k_{zs} f H / U_H / (2.5 + \beta'_s)}{1 + k_{zs} f H / U_H / (2.5 + \beta_s)}} \quad (15)$$

where H = building height; Θ_{js0} = value of the mode shape at the building top; β_s = mode shape exponent; \bar{P}_{s0} and $S_{P_{s0}}(f)$ = mean and PSD of wind load at the building top floor; k_{zs} = decay factor; U_H = mean wind speed at the building top; α_{s0} and α_s = mean and dynamic wind load profile exponents. When the actual building mode shape can not be adequately fitted by a power law, the mode shape correction can be directly obtained by its definition in Eqs. (9) and (10) using the actual mode shape values for an assumed dynamic wind load distribution. Regardless of whether the actual building mode shapes can be adequately approximated by a power law, the actual mode shapes should be used with the best estimates of the dynamic response and the equivalent static load.

It is also noteworthy that when the frequency dependent modal shape corrections are simplified as independent of frequency, Eq. (8) is equivalent to the following expression for $Q_j(t)$ ($j=1, 2, 3$) (e.g., Irwin and Xie 1993; Holmes et al. 2003):

$$Q_j(t) = \eta_{jx} M_x(t) + \eta_{jy} M_y(t) + \eta_{j\theta} M_\theta(t) \quad (16)$$

Coupled Response Analysis

The mean, root-mean-square (RMS) background and resonant components of the j th generalized displacement, \bar{q}_j , $\sigma_{q_{jb}}$, and $\sigma_{q_{jr}}$, are given by

$$\bar{q}_j = \frac{\bar{Q}_j}{K_j} \quad (17)$$

$$\sigma_{q_{jb}}^2 = \int_0^{f'} |H_j(f)|^2 S_{Q_{jj}}(f) df \approx \frac{1}{K_j^2} \int_0^\infty S_{Q_{jj}}(f) df \quad (18)$$

$$\sigma_{q_{jr}}^2 = \int_{f'}^\infty |H_j(f)|^2 S_{Q_{jj}}(f) df \approx \frac{1}{K_j^2} \frac{\pi}{4 \xi_j} f_j S_{Q_{jj}}(f_j) \quad (19)$$

$$H_j(f) = \frac{1}{K_j[1 - (f/f_j)^2 + 2i\xi_j f/f_j]} \quad (20)$$

$$K_j = (2\pi f_j)^2 \sum_{k=1}^N (m_k \Theta_{kjxc}^2 + m_k \Theta_{kjyc}^2 + I_k \Theta_{kj\theta c}^2) \quad (21)$$

where K_j , f_j , and ξ_j = j th generalized stiffness, modal frequency, and damping ratio; $\Theta_{kjxc} = \Theta_{kix} - e_{ky} \Theta_{kj\theta}$, $\Theta_{kjyc} = \Theta_{kij} + e_{kx} \Theta_{kj\theta}$ and $\Theta_{kj\theta c} = \Theta_{kj\theta}$ = j th mode shape in terms of the motions at the mass center of the k th floor; $f' \leq f_1$; and $i = \sqrt{-1}$.

The covariance between the background components of the j th and k th modal responses, $\sigma_{kjb}^2 = \sigma_{kjb}^2$, is expressed as

$$\sigma_{kjb}^2 = \text{Re} \left[\int_0^{f'} H_j(f) H_k^*(f) S_{Q_{jk}}(f) df \right] = r_{jkb} \sigma_{q_{jb}} \sigma_{q_{kb}} \quad (22)$$

$$r_{jkb} \approx \frac{\int_0^\infty \text{Re}[S_{Q_{jk}}(f)] df}{\sqrt{\int_0^\infty S_{Q_{jj}}(f) df} \sqrt{\int_0^\infty S_{Q_{kk}}(f) df}} = \frac{\sigma_{Q_{jk}}^2}{\sigma_{Q_{jj}} \sigma_{Q_{kk}}} = r_{Q_{jk}} \quad (23)$$

where r_{jkb} and $r_{Q_{jk}}$ =modal correlation coefficients of the j th and k th background modal responses and generalized forces, respectively; Re and superscript * represent the real and complex conjugate operators, respectively.

The covariance between the resonant components of the j th and k th modal responses, $\sigma_{q_{jkr}}^2 = \sigma_{q_{jkr}}^2$, is given by

$$\sigma_{q_{jkr}}^2 = \text{Re} \left[\int_{f'}^\infty H_j(f) H_k^*(f) S_{Q_{jk}}(f) df \right] = r_{jkr} \sigma_{q_{jr}} \sigma_{q_{kr}} \quad (24)$$

where r_{jkr} =correlation coefficient of the j th and k th resonant modal responses, which can be approximated by the following closed-form expressions (Chen and Kareem 2005a):

$$r_{jkr} = \alpha_{jkr} \rho_{jkr} \quad (25)$$

$$\alpha_{jkr} = \text{Re}[S_{Q_{jk}}(f)] / \sqrt{S_{Q_{jj}}(f) S_{Q_{kk}}(f)}|_{f=f_j \text{ or } f_k} \quad (26)$$

and ρ_{jkr} is given in Der Kiureghian (1980)

$$\rho_{jkr} = \frac{8\sqrt{\xi_j \xi_k} (\beta_{jk} \xi_j + \xi_k) \beta_{jk}^{3/2}}{(1 - \beta_{jk}^2)^2 + 4\xi_j \xi_k \beta_{jk} (1 + \beta_{jk}^2) + 4(\xi_j^2 + \xi_k^2) \beta_{jk}^2} \quad (27)$$

where $\beta_{jk} = f_j/f_k$ with $0 \leq \beta_{jkr} \leq 1$; $\rho_{jkr} = \rho_{kkr} = 1$; and $\rho_{jkr} = \rho_{jkr} \ll 1$ when f_j , and f_k are well separated. It is worth mentioning that the parameter α_{ijr} represents the partially correlated feature of the generalized forces $Q_j(t)$ and $Q_k(t)$. In general, $|\alpha_{ijr}| \leq 1$, and only when the generalized forces are fully correlated, $|\alpha_{ijr}| = 1$. This important consideration for the accurate utilization of the CQC scheme has not been completely recognized for the analysis of wind load effects on buildings and structures (e.g., Xie et al. 2003).

The generalized dynamic displacement including the background and resonant components is given by

$$\sigma_{q_j} = \sqrt{\sigma_{q_{jb}}^2 + \sigma_{q_{jr}}^2} \quad (28)$$

and the correlation coefficient for the j th and k th modal responses (including the background and resonant components) is thus expressed as

$$r_{jk} = \frac{\sigma_{q_{jk}}}{\sigma_{q_j} \sigma_{q_k}} = \frac{r_{jkb} \sigma_{q_{jb}} \sigma_{q_{kb}} + r_{jkr} \sigma_{q_{jr}} \sigma_{q_{kr}}}{(\sqrt{\sigma_{q_{jb}}^2 + \sigma_{q_{jr}}^2})(\sqrt{\sigma_{q_{kb}}^2 + \sigma_{q_{kr}}^2})} \quad (29)$$

Any response of interest, e.g., displacement, bending moment, shear force, and other member forces at any elevations can be quantified from the generalized displacements. Considering a specific response, R , its mean and RMS dynamic components can be expressed as

$$\bar{R} = \sum_{j=1}^3 \bar{R}_j = \sum_{j=1}^3 \Gamma_j \bar{q}_j \quad (30)$$

$$\sigma_R^2 = \sum_{j=1}^3 \sum_{k=1}^3 \sigma_{R_j} \sigma_{R_k} r_{jk} = \sum_{j=1}^3 \sum_{k=1}^3 \Gamma_j \Gamma_k \sigma_{q_j} \sigma_{q_k} r_{jk} \quad (31)$$

where $\sigma_{R_j} = \Gamma_j \sigma_{q_j}$; and Γ_j = j th modal participation coefficient for R , representing the static response of R under the modal inertial load with a unit generalized displacement

$$\Gamma_j = \sum_{i=1}^N (\mu_{ixc} F_{ijxc0} + \mu_{iyc} F_{ijyc0} + \mu_{i\theta c} F_{ij\theta c0}) \quad (32)$$

$$F_{ijsc0} = (2\pi f_j)^2 m_{is} \Theta_{ijsc} \quad (s = x, y, \theta) \quad (33)$$

$\mu_{isc}(z)$ ($s = x, y, \theta$)=influence function representing the response R under a unit load acting at the mass center of the i th floor along the s direction; F_{ijsc0} ($i = 1, 2, \dots, N; s = x, y, \theta$)= j th modal inertial load with a unit generalized displacement acting at the mass center; and $m_{ix} = m_{iy} = m_i$ and $m_{i\theta} = I_i$.

It is evident that for the displacement, velocity, and acceleration at the mass center of the i th floor in the axis s direction, Γ_j can be respectively given by Θ_{ijsc} , $(2\pi f_j) \Theta_{ijsc}$ and $(2\pi f_j)^2 \Theta_{ijsc}$. For shear, bending moment and torque (about axis z) at the i th floor, Γ_j can be, respectively, expressed as

$$\Gamma_j = \sum_{k=i+1}^N (2\pi f_j)^2 m_k \Theta_{kjsc} \quad (s = x, y) \quad (34)$$

$$\Gamma_j = \sum_{k=i+1}^N (z_k - z_i) (2\pi f_j)^2 m_k \Theta_{kjsc} \quad (s = x, y) \quad (35)$$

$$\Gamma_j = \sum_{k=i+1}^N (2\pi f_j)^2 (-m_k e_{ky} \Theta_{kjxc} + m_k e_{kx} \Theta_{kjyc} + I_k \Theta_{kj\theta c}) \quad (36)$$

The correlation coefficient between two responses, R and D , is given by

$$r_{RD} = \frac{\mu_{RD}}{\sigma_R \sigma_D} \quad (37)$$

$$\mu_{RD} = \sum_{j=1}^3 \sum_{k=1}^3 \Gamma_j \Gamma_k \sigma_{q_j} \sigma_{q_k} r_{jk} \quad (38)$$

where σ_D =RMS of response D and given by Eq. (31) with Γ_{kD} for replacing Γ_k ; and Γ_{kD} = k th modal participation coefficient for D .

It is noted that when the inter-modal coupling among modal responses can be neglected, i.e., $r_{jk}=1$ for $j=k$ and $r_{jk}=0$ for $j \neq k$, the CQC rule given by Eqs. (31) and (38) reduces to the square root of the sum of squares (SRSS) rule.

The mean peak response of R including the mean and fluctuating components is given as $\bar{R} \pm g\sigma_R$, where g =the peak factor, generally ranging between 3 and 4.

It should be noted that the mean and background components of the base bending moments and torque, \bar{M}'_s and M'_s (where the prime is used to distinguish the response from the respective load component), are identical to the measured integrated loads, \bar{M}_s and M_s ($s=x,y,\theta$). This leads to an alternative procedure for quantifying the mean and background generalized displacements without introducing any mode shape correction procedure

$$\{\bar{q}\} = [\Gamma]^{-1}\{\bar{M}\} \quad (39)$$

$$[\sigma_{q_b}^2] = [\Gamma]^{-1}[\sigma_M^2][\Gamma]^{-T} \quad (40)$$

where $[\sigma_{q_b}^2] = [\sigma_{q_{jkb}}^2]$; $[\Gamma] = [\Gamma_{jM_s}]$; Γ_{jM_s} = j th modal participation coefficient for M'_s ; and $\{\bar{M}\}$ and $[\sigma_M^2]$ =mean and covariance matrix of the measured base bending moments and torque.

Equivalent Static Wind Loads

The HFFB measurements do not provide information regarding the spatial distribution of wind loads. When the mean load distribution is unavailable, a viable approximation for tall buildings to model the mean wind loads is described by the sum of the modal inertial loads associated with the mean modal responses \bar{q}_j ($j=1,2,3$)

$$\bar{F}_{isc} = \bar{F}_{i1sc} + \bar{F}_{i2sc} + \bar{F}_{i3sc} \quad (s=x,y,\theta) \quad (41)$$

$$\bar{F}_{ijsc} = (2\pi f_j)^2 m_{is} \Theta_{ijsc} \bar{q}_j \quad (j=1,2,3) \quad (42)$$

where \bar{F}_{isc} and \bar{F}_{ijsc} =mean and j th modal inertial loads acting on the mass center of the i th floor along the axis s direction. It is noted that while this load distribution is generally different from the actual mean load, it results in an accurate estimate of the mean response quantified through the modal analysis involving only the fundamental modes.

It is straightforward to express the ESWL for the j th modal peak response, $R_{jmax} = g\sigma_{R_j} = g\Gamma_j\sigma_{q_j}$, as the peak modal inertial load, which is independent of response considered

$$F_{ijsc} = (2\pi f_j)^2 m_{is} \Theta_{ijsc} g\sigma_{q_j} \quad (s=x,y,\theta) \quad (43)$$

The ESWL for the total peak response, $g\sigma_R$, cannot simply be expressed as the sum of the peak modal inertial loads for $g\sigma_{R_j}$ ($j=1,2,3$), or by their combination using the SRSS or CQC rules. Current design practice often expresses the ESWL for the total peak response as a linear combination of the peak modal inertial loads with adequately defined weighting/combination factors. Similar treatment is exercised in the combination of alongwind, acrosswind, and torsional loads for combined actions of buildings with uncoupled modes. For buildings with one-dimensional uncoupled modes, the peak modal inertial loads associated with each mode can be regarded as the distribution of base bending moments or base torque over the building height. Accordingly, the ESWL for any peak response of the combined action contributed by multimodes can be regarded as a linear combination of the integrated wind loads in terms of base bending moments and torque.

There are infinite combinations of peak modal inertial loads for the ESWL associated with the total peak response. However,

the following combination scheme leads to a most probable load distribution (Boggs and Peterka 1989; Chen and Kareem 2001 and 2005a; Holmes 2002):

$$F_{eRisc} = W_{1R}F_{i1sc} + W_{2R}F_{i2sc} + W_{3R}F_{i3sc} \quad (s=x,y,\theta) \quad (44)$$

$$W_{jR} = \left(\sum_{k=1}^3 \sigma_{R_k} r_{jk} \right) / \sigma_R \quad (j=1,2,3) \quad (45)$$

The weighting factor W_{jR} ($j=1,2,3$)=function of the modal correlation coefficients and the ratios of modal response components. Therefore, these generally depend on the individual response. The total ESWL for the peak response $\bar{R} \pm g\sigma_R$ is accordingly given by $\bar{F}_{isc} \pm F_{eRisc}$.

Consider the dynamic response contributed by two modes, e.g., the first two modes. According to Eq. (45), the weighting factors become

$$W_{1R} = \frac{1 + (\sigma_{R_2}/\sigma_{R_1})r_{12}}{\sqrt{1 + (\sigma_{R_2}/\sigma_{R_1})^2 + 2r_{12}(\sigma_{R_2}/\sigma_{R_1})}} \quad (46)$$

$$W_{2R} = \frac{r_{12} + (\sigma_{R_2}/\sigma_{R_1})}{\sqrt{1 + (\sigma_{R_2}/\sigma_{R_1})^2 + 2r_{12}(\sigma_{R_2}/\sigma_{R_1})}} \quad (47)$$

For the case in which $\sigma_{R_1} = \sigma_{R_2}$ and $r_{12} = 0$, it results in $W_{1R} = W_{2R} = 0.707$, which corresponds to the combination factor of 0.75 adopted in ASCE 7-02 standard and NBCC code, and it is referred to as 75% rule in the following discussion.

Alternatively, the following combinations can be defined:

$$W_{1R}^{(1)} = 1 \quad (48)$$

$$W_{2R}^{(1)} = [\sqrt{1 + (\sigma_{R_2}/\sigma_{R_1})^2 + 2r_{12}(\sigma_{R_2}/\sigma_{R_1})} - 1](\sigma_{R_1}/\sigma_{R_2})$$

$$W_{1R}^{(2)} = [\sqrt{1 + (\sigma_{R_1}/\sigma_{R_2})^2 + 2r_{12}(\sigma_{R_2}/\sigma_{R_1})} - 1](\sigma_{R_2}/\sigma_{R_1}) \quad (49)$$

$$W_{2R}^{(2)} = 1$$

When $\sigma_{R_1} = \sigma_{R_2}$, Eqs. (48) and (49) lead to

$$W_{2R}^{(2)} = W_{1R}^{(1)} = \sqrt{2 + 2r_{12}} - 1 \quad (50)$$

which corresponds to the combination rule that takes into account the modal correlation as adopted in *AIJ-RLB-2004* (Asami 2000; Tamura et al. 2003a). By further setting $r_{12} = 0$, it leads to $W_{2R}^{(2)} = W_{1R}^{(1)} \approx 40\%$, i.e., the 40% rule, which has been widely adopted in building codes for earthquake loadings.

These simplified combination rules eliminate the dependence of the weighting factors on the individual response, and further on the modal correlation coefficient. Their performance can be investigated by comparing their estimates with those according to the CQC rule for different r_{12} and $c_{12} = \sigma_{R_2}/\sigma_{R_1}$. The combination rule that takes into account the modal correlation leads to more conservative results than the CQC rule, and offers a better performance than the 40 and 75% rules, provided the modal correlation coefficient can be adequately estimated. The 40 and 75% rules result in very conservative estimates in some cases but nonconservative in others. For example, for $r_{12} = -0.6$ and $c_{12} = 1$, or for $r_{12} = 0.6$ and $c_{12} = -1$, the response ratios with respect to CQC rule are 1.57 and 1.68, respectively, for the 40 and 75% rules, which means an overestimate of the response. On the other hand, for

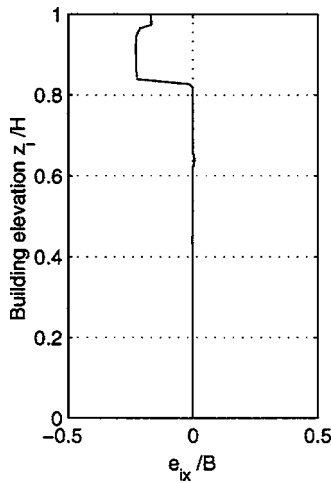


Fig. 2. Coincident centers of mass and resistance at different floors

$r_{12}=0.6$, and $c_{12}=1$, or for $r_{12}=-0.6$, and $c_{12}=-1$, the response ratios are 0.78 and 0.84, respectively, which means underestimation of the response.

Application and Discussion

Coupled Building Response

A building approximately 450 m in height is considered as an example to illustrate the analysis framework presented in this study. The building footprint at the base is about 72 m \times 72 m. This cross section is reduced in steps to about 24 m \times 48 m at the upper levels. The coordinate system is defined in Fig. 1 with the origin at the center of the base footprint. Due to setbacks at upper floors in the negative x direction, the centers of mass and resistance, though coinciding at each floor, do not lie on a single vertical axis as shown in Fig. 2 for e_{ix}/B with $e_{iy}/B=0$. As a result, the building exhibits 3D coupled mode shapes, particularly, strong coupled motion in two translational directions is observed. As shown in Fig. 3, the first and second fundamental modes are, respectively, dominated by the out-of-phase and in-phase coupled translational motions, indicating that the building approximately vibrates in the orthogonal diagonal directions of the building plan. As the principle axes of the translational motions are not identical over the building height, these modes can not be simply regarded as one dimensional uncoupled modes with motions restricted to principle directions. The third mode is dominated by the torsional

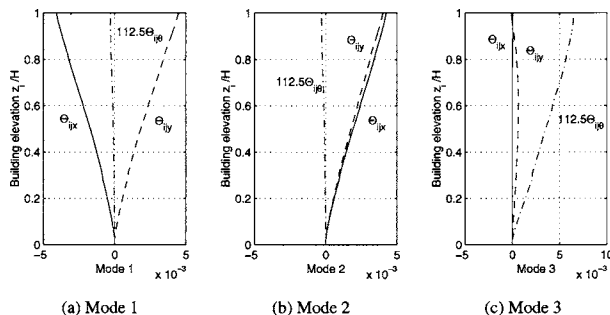


Fig. 3. Coupled mode shapes of fundamental modes

motion. The frequency ratios are $f_2/f_1=1.023$ and $f_3/f_1=1.7442$. The damping ratio for each mode is assumed to be 1%.

The HFFB measurements at different wind directions over 360° with an interval of 10° were conducted in a large cross-section boundary layer wind tunnel under simulated urban wind environments in which the surrounding buildings were also modeled to consider the local flow field distortion. These measurements include base bending moments in translational x and y directions and torque around the vertical axis z . As indicated in Fig. 1, $\alpha=0^\circ$ for wind blowing from the positive y direction, and $\alpha=90^\circ$ for wind blowing from the positive x direction.

To estimate the mode shape corrections required in the estimation of the generalized forces, the building mode shapes were approximated by a power law and the mode shape corrections, were based on fully correlated wind load case. For some mode components, e.g., the translational motion in the y direction in mode 3, Θ_{13y} , instead of fitting the mode shapes as a power law, the mode shape corrections were directly based on the actual mode shapes. The mode shape corrections used in this example are assumed as independent of frequency and wind direction. These are: $\eta_{1x}/(\Theta_{1x0}/H)=\eta_{2x}/(\Theta_{2x0}/H)=\eta_{1y}/(\Theta_{1y0}/H)=\eta_{2y}/(\Theta_{2y0}/H)=0.86$; $\eta_{1\theta}/\Theta_{100}=\eta_{2\theta}/\Theta_{200}=0.52$; $\eta_{3x}/(\Theta_{3x0}/H)=1.08$; $\eta_{3y}/(\Theta_{3y0}/H)=1.23$; $\eta_{3\theta}/\Theta_{300}=0.56$, where Θ_{is0} ($i=1,2,3$; $s=x,y,\theta$) are the mode shapes at the building top determined from the curve-fitted power laws. It is important to note that those approximated mode shapes expressed as power laws are only used for the quantification of mode shape corrections. The actual mode shapes should be utilized in the response analysis. The mean response is directly estimated from the base forces without introducing mode shape corrections. The modal participation coefficients for M'_x , M'_y , and M'_θ are: $(\Gamma_{1M_x}, \Gamma_{2M_x}, \Gamma_{3M_x})/\Gamma_{2M_x}=(-0.8831, 1.0, -0.0065)$; $(\Gamma_{1M_y}, \Gamma_{2M_y}, \Gamma_{3M_y})/\Gamma_{2M_y}=(0.9488, 0.9269, 0.2693)$; $(\Gamma_{1M_\theta}, \Gamma_{2M_\theta}, \Gamma_{3M_\theta})/\Gamma_{1M_x}=(-0.0115, -0.0115, 0.5108)$. Similarly, for the combined action, $M'_{xy1}=(M'_x+M'_y)/\sqrt{2}$, these are $(\Gamma_{1M_{xy1}}, \Gamma_{2M_{xy1}}, \Gamma_{3M_{xy1}})/\Gamma_{2M_x}=(0.0464, 1.3625, 0.1859)$.

The mean, maximum and minimum base bending moments and torque responses, \bar{M}'_s , $\bar{M}'_s+3.8\sigma_{M'_s}$ and $\bar{M}'_s-3.8\sigma_{M'_s}$ ($s=x,y,\theta$), for the 50 year return period wind event, are plotted against varying wind azimuth in Fig. 4. These are expressed in terms of the nondimensional force coefficients which are defined by the bending moment and base torque normalized by $0.5\rho U^2 B H^2$ and $0.5\rho U^2 B^2 H$, respectively. The 50 year return period wind speed is determined irrespective of the wind direction. In Fig. 4, the maximum and minimum values without the resonant component, i.e., mean+background response, are identical to those directly obtained from the HFFB measurements when the scheme in Eq. (40) is applied. It is noted that \bar{M}'_x reaches its largest positive and negative values as α approaches about 270 and 90°, respectively. \bar{M}'_y reaches its largest extremes as α approaches about 180 and 0°. Both correspond to the alongwind excitations. \bar{M}'_θ is relatively small with positive and negative peaks at about 200 and 0°, which are considered to be related to the alongwind loads in the y direction acting on the higher floors with a setback in the negative x direction. The maximum and minimum response, including the mean, background and resonant components, are observed around $\alpha=280$ and 70° for M'_x , around $\alpha=180$ and 0° for M'_y . Both the maximum and minimum values of M'_θ are observed around $\alpha=160^\circ$, which are dominated by the

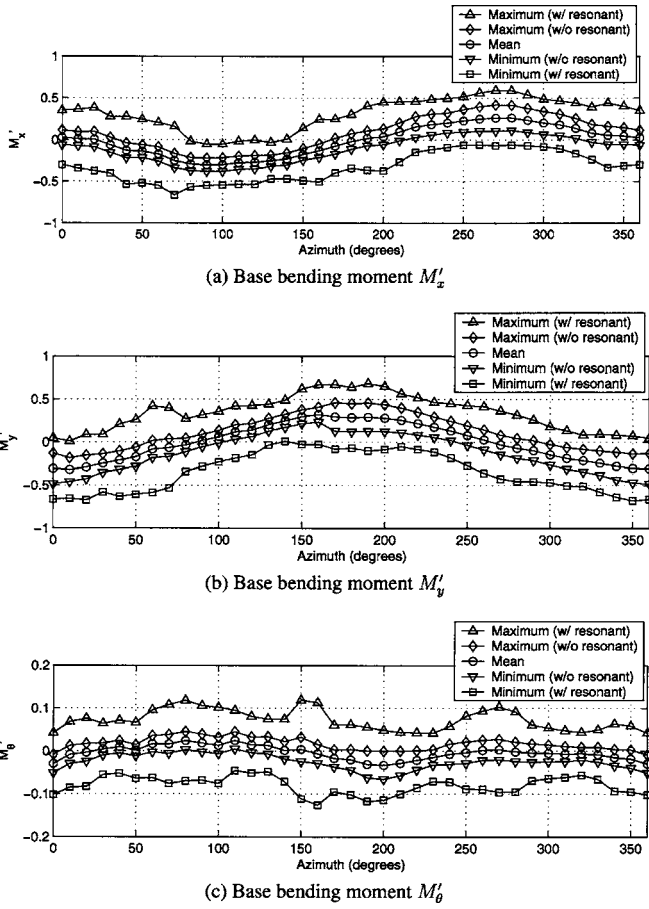


Fig. 4. Mean, maximum, and minimum response

resonant component. It is evident that the peak values of different response components are generally observed at different wind directions.

Role of Cross Correlation of Wind Loads

The variation of cross-correlation coefficients between measured base bending moments and torque with wind direction is shown in Fig. 5, which also represent the cross correlations of integrated loads in the three primary directions. As expected, M_x and M_y have relatively higher correlation when wind directions are not perpendicular to the side faces of the building. Due to the presence of the setbacks at higher floors in the negative x direction, M_θ is more correlated with M_y in comparison with M_x .

For uncoupled buildings with 1D mode shapes, the cross correlation of wind loads does not affect the building response in the

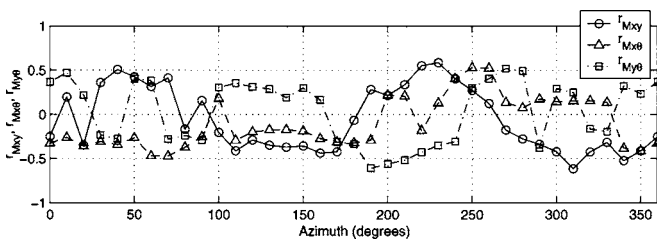


Fig. 5. Correlation coefficients between integrated wind loads in terms of base bending moments and torque

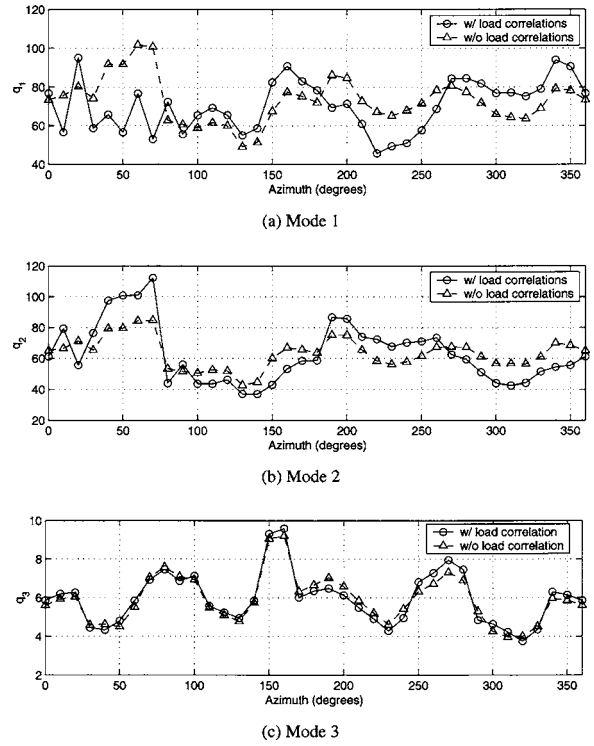
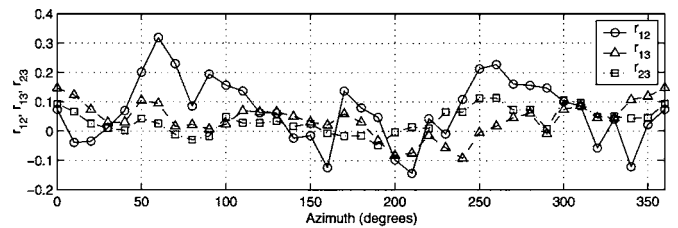
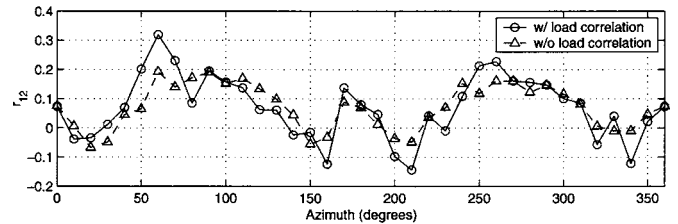


Fig. 6. Root mean square generalized displacements

primary directions, although it affects their correlation thus their combined actions. However, for coupled buildings with 3D mode shapes and closely spaced mode frequencies, it influences both the modal responses and their correlations thus the overall building response. Each response component exhibits a different level of sensitivity to the wind correlation. For example, the RMS modal response, modal response correlation coefficients and RMS M'_x , M'_y , and M'_{xy1} are shown in Figs. 6–8. As expected, the response components associated with the first and second modes are remarkably affected, while those dominated by the third mode are almost unaffected. For example, the response ratios between the cases without and with the load correlation at wind directions



(a) r_{12} , r_{13} and r_{23}



(b) r_{12} with and without cross-correlation of wind loads

Fig. 7. Modal correlation coefficients

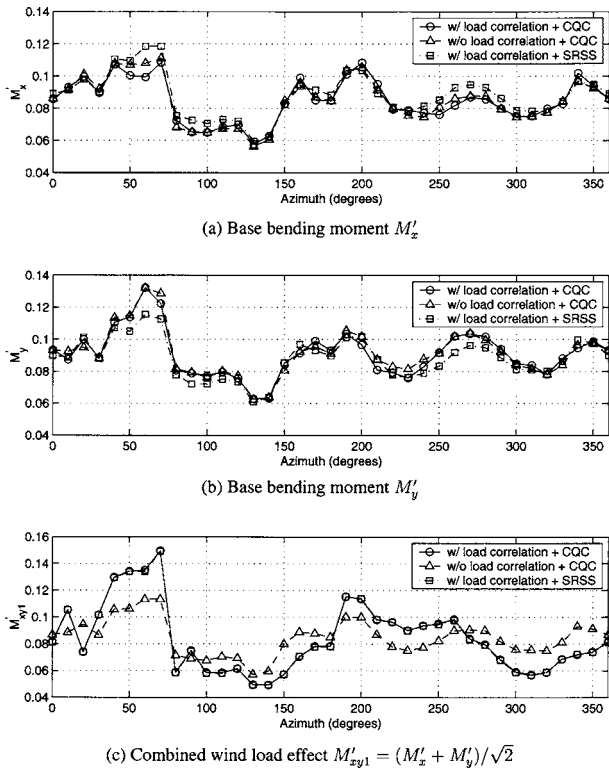


Fig. 8. Root mean square base bending moments and combined actions

$\alpha=70^\circ$ and 310° are: for M'_x , 1.0243 and 0.9981; for M'_y , 1.0512 and 0.9729; for M'_{xy1} , 0.7571 and 1.3278, respectively.

It is noted that the modal correlation coefficients vary with wind direction due to the contribution of the partially correlated generalized forces [Eq. (25)]. As expected, the first two modes exhibit stronger correlation due to their closely spaced frequencies. The cross correlation of wind loads results in the highest modal correlation at $\alpha=60^\circ$ for this example building.

Each response corresponds to a unique set of modal participation coefficients. Therefore, the influence of wind correlation on different response components can be investigated by changing the ratios of these modal participation coefficients, Γ_2/Γ_1 and Γ_3/Γ_1 . In Fig. 9, the results for the response contributed by the first two modes, expressed as the response ratios between the cases without and with the wind load correlation, are plotted as functions of Γ_2/Γ_1 , and wind direction, α . It can be seen that building response dominated by a single mode of the first two modes, such as M'_{xy1} , may be significantly over- or underesti-

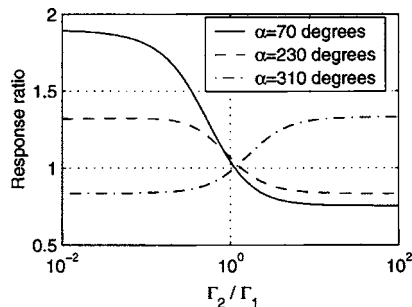


Fig. 9. Influence of cross correlation of wind loads on response

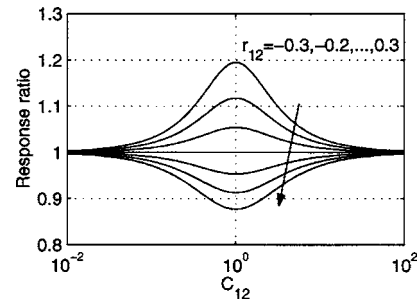


Fig. 10. Influence of modal correlation on response

mated without the consideration of cross-wind correlations of wind loads. On the other hand, the response which is almost equally contributed by the first two modes such as M'_x and M'_y is insensitive to the wind load correlation.

Role of Correlation of Modal Response

The influence of modal response correlation (inter-modal coupling) on RMS M'_x , M'_y , and M'_{xy1} is shown in Fig. 8. The SRSS and CQC rules correspond to the calculations without and with the modal response correlations. It can be seen that the modal correlation has noteworthy influence on the base bending moments in the wind directions in which the responses of Modes 1 and 2 are significantly correlated, i.e., around $\alpha=70^\circ$ and 270° . At 70° , the ratio of response by SRSS to that by CQC is 1.0935 for M'_x , 0.9204 for M'_y , and 0.9964 for M'_{xy1} .

The results for different RMS response components, which are contributed by the first two modes, are shown in Fig. 10. These are the ratios of the response by SRSS rule to that by CQC rule, and expressed as a function of the ratio of the modal contributions, $c_{12}=\Gamma_2\sigma_{q2}/(\Gamma_1\sigma_{q1})$, and the modal correlation coefficient, r_{12} . It is noted that response which is almost equally contributed by the first two modes may be significantly over- or underestimated without the consideration of correlation of modal responses at wind directions at which modal responses are highly correlated.

The influence of wind load correlation and modal response correlation on the building accelerations at the roof level in a 10 year return period wind event is shown in Fig. 11. It is similar

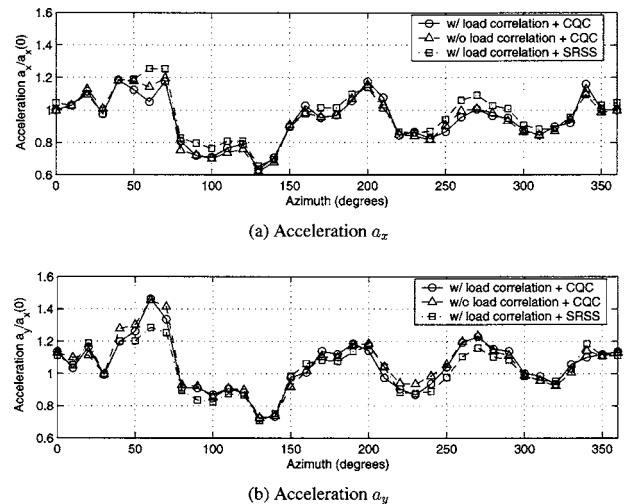


Fig. 11. Root mean square accelerations at building top

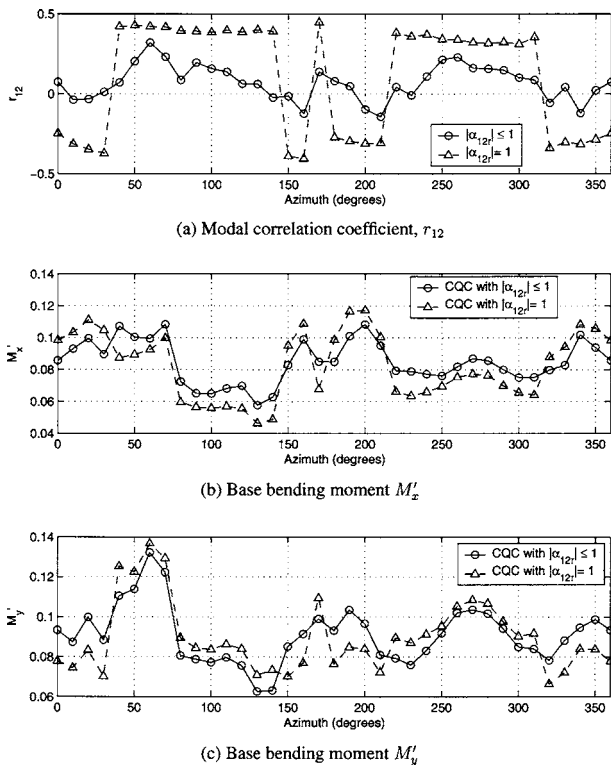


Fig. 12. Influence of modal correlation coefficient on base bending moments

to the observations made for the base bending moments.

An accurate quantification of the modal response correlation coefficients is important for response prediction by the CQC scheme. The partially correlated feature of wind loads needs to be addressed in the closed-form formulations of the CQC scheme in terms of the parameter α_{ijr} with $|\alpha_{ijr}| \leq 1$, in general. However, it has often been ignored by implicitly assuming $|\alpha_{ijr}| = 1$ in literature (e.g., Xie et al. 2003). Figs. 12 and 13 show the influence of approximation of α_{ijr} (where $i=1$ and $j=2$) on the modal correlation coefficient of the translational modes, and on the RMS values of the base bending moments. These results clearly demonstrate the importance of considering the partially correlated feature of wind loads for accurate predictions of wind load effects on structures.

Comments on Building Response Correlation

The correlation coefficients of building base bending moments and torque responses, i.e., M'_x , M'_y , and M_θ , are shown in Fig. 13. Compared to the correlation of the respective integrated wind

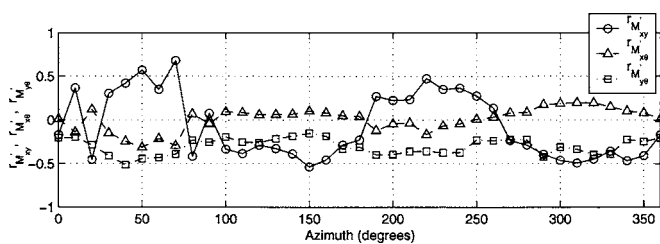


Fig. 13. Correlation coefficients of base bending moments and torque responses

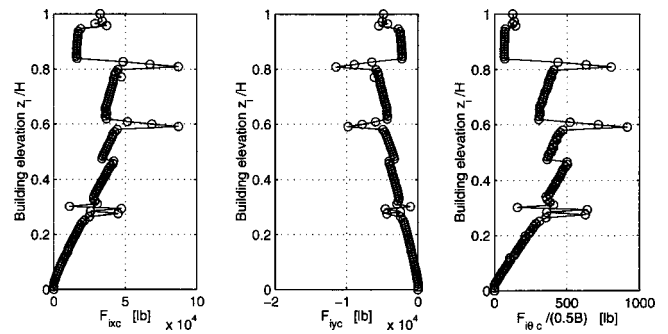


Fig. 14. Equivalent mean wind load distributions (270°)

loads, i.e., M_x , M_y , and M_θ , as shown in Fig. 5, the correlation between M'_x and M'_y shows similar variation as M_x and M_y , while correlation between M'_x and M'_θ , and between M'_y and M'_θ become distinctly different, in particular M'_x and M'_θ become almost uncorrelated, due to the fact that they are, respectively, contributed from almost uncorrelated modes. It should be emphasized that the correlation coefficients of the base bending moments and torque responses are generally distinct from those of the respective integrated loads. For example, in the case of uncoupled buildings with well separated mode frequencies and dominant resonant modal responses, the building response components in different primary directions are expected to be almost uncorrelated despite the presence of strong correlation among the integrated loads.

While for uncoupled buildings with 1D mode shapes the correlation coefficients of the base bending moments and torque responses are identical to those of the modal responses, this is not necessarily true for coupled buildings with 3D mode shapes. Better understanding of this distinction is important in dealing with the combination of loads on tall buildings, where the correlation of modal responses is required rather than the correlation of integrated loads. Nonetheless, a commentary on the correlation of integrated loads also helps in better understanding the background loads and associated response (Tamura et al. 2003b).

Equivalent Static Wind Loads

The mean load distributions approximated by the sum of the modal inertial loads are shown in Fig. 14 at $\alpha = 270^\circ$ which corresponds to the maximum value of \bar{M}'_x . The mean load is independent of response considered. Under the action of this mean load, any mean response for the same wind direction can be determined through a static analysis.

The first peak modal inertial load distribution at $\alpha = 270^\circ$ is shown in Fig. 15. The peak modal inertial loads associated with other modes can be similarly obtained but have not been shown here for the sake of brevity. Under these peak modal inertial loads, any response component at the same wind direction and speed can be predicted by utilizing a static analysis procedure and the CQC rule. A number of ESWLs associated with important response components at different critical wind directions can be conveniently obtained by following the framework presented here for building design applications.

Concluding Remarks

The analysis of coupled response and modeling of equivalent static wind loads on tall buildings with 3D modes based on the

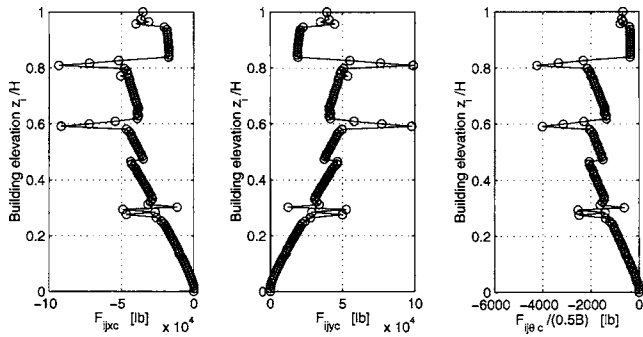


Fig. 15. Peak modal inertial load distributions (second mode, 270°)

HFFB measurements was studied. Both the mean and fluctuating responses were calculated by the modal analysis involving three fundamental modes. Formulations for the prediction of the generalized wind forces with mode shape corrections, generalized displacements, and any response of interest were presented with a focus on buildings whose mass centers may not align in a single vertical axis. The proposed framework took into account the cross correlation of wind loads acting in different primary directions and the intermodal coupling of modal responses with closely spaced modal frequencies. The ESWL for a given peak response of interest was given in terms of modal inertial loads. The combination rules for these modal inertial loads were investigated.

The tall building example with 3D coupled modes delineated the significance of the cross correlation of wind loads and the intermodal coupling of modal responses in the accurate prediction of coupled building response. Results indicated that different response components have different sensitivity to the cross correlation of wind loads and the intermodal coupling. The coupled responses may be significantly over- or underestimated when the influence of the cross correlation of wind loads and the intermodal coupling was neglected.

The proper role of the correlation between integrated loads, modal responses, and respective building response components in the evaluation of wind effects on coupled buildings has been elucidated. A clear understanding of their distinction is quintessential in the treatment of load combinations on tall buildings, where the correlation of modal responses is required rather than the correlation of integrated loads often implied in the literature. This study offers a versatile analysis framework which would help in better understanding the coupled building response to spatiotemporally varying dynamic wind loads.

Acknowledgments

The support for this work provided in part by NSF Grant No. CMS 03-24331 is gratefully acknowledged. The first author also gratefully acknowledges the support of the new faculty startup funds provided by the Texas Tech University.

References

American Society of Civil Engineers (ASCE). (2002). "Minimum design loads for buildings and other structures." *ASCE 7-02*, New York.
 Asami, Y. (2000). "Combination method for wind loads on high-rise buildings." *Proc., 16th National Symp. on Wind Engineering*, Japan

Association for Wind Engineering (JAWE), Tokyo, 531–534 (In Japanese).
 Boggs, D. W., and Peterka, J. A. (1989). "Aerodynamic model tests of tall buildings." *J. Eng. Mech.*, 115(3), 618–635.
 Chen, X., and Kareem, A. (2001). "Equivalent static wind loads for buffeting response of bridges." *J. Struct. Eng.*, 127(12), 1467–1475.
 Chen, X., and Kareem, A. (2004a). "Coupled building response analysis using HFFB: Some new insights." *Proc., 5th Bluff Body Aerodynamics and Applications (BBAAV)*, Ottawa.
 Chen, X., and Kareem, A. (2004b). "Equivalent static wind loads on buildings: New model." *J. Struct. Eng.*, 130(10), 1425–1435.
 Chen, X., and Kareem, A. (2005a). "Coupled dynamic analysis and equivalent static wind loads on buildings with 3-D modes." *J. Struct. Eng.*, 131(7), 1071–1082.
 Chen, X., and Kareem, A. (2005b). "Validity wind load distribution based on high frequency force balance measurements." *J. Struct. Eng.*, 131(6), 984–987.
 Davenport, A. G. (1967). "Gust loading factors." *J. Struct. Div. ASCE*, 93, 11–34.
 Davenport, A. G. (1985). "The representation of the dynamic effects of turbulent wind by equivalent static wind loads." *Proc., AISC/CISC International Symp. on Structural Steel*, Chicago, 3-1–3-13.
 Der Kiureghian, A. (1980). "Structural response to stationary excitation." *J. Eng. Mech. Div.*, 106(6), 1195–1213.
 Flay, R. G. J., Yip, D. Y. N., and Vickery, B. J. (1999). "Wind induced dynamic response of tall buildings with coupled 3D modes of vibration." *Proc., 10th International Conf. on Wind Engineering*, Copenhagen, Denmark, 645–652.
 Holmes, J. D. (2002). "Effective static load distributions in wind engineering." *J. Wind. Eng. Ind. Aerodyn.*, 90, 91–109.
 Holmes, J. D., Rofail, A., and Aurelius, L. (2003). "High frequency base balance methodologies for tall buildings with torsional and coupled resonant modes." *Proc., 11th International Conf. on Wind Engineering*, Texas Tech Univ., Lubbock, Tex., 2381–2388.
 Irwin, P. A., and Xie, J. (1993). "Wind loading and serviceability of tall buildings in tropical cyclone regions." *Proc., 3rd Asia-Pacific Symp. on Wind Engineering*, Univ. of Hong Kong, Hong Kong.
 Islam, S., Ellingwood, B., and Corotis, R. B. (1992). "Wind-induced response of structurally asymmetric high-rise buildings." *J. Struct. Eng.*, 118(1), 207–222.
 Kareem, A. (1985). "Lateral-torsional motion of tall buildings." *J. Struct. Eng.*, 111(11), 2479–2496.
 Kareem, A., and Cermak, J. E. (1979). "Wind tunnel simulation of wind-structure interactions." *ISA Trans.*, 18(4), 23–41.
 Kareem, A., and Zhou, Y. (2003). "Gust loading factors—past, present and future." *J. Wind. Eng. Ind. Aerodyn.*, 91(12–15), 1301–1328.
 Kasperski, M. (1992). "Extreme wind load distributions for linear and nonlinear design." *Eng. Struct.*, 14, 27–34.
 Melbourne, W. H. (1975). "Probability distributions of response of BHP house to wind action and model comparisons." *J. Wind Ind. Aerodyn.*, 1(2), 167–175.
 National Building Code of Canada (NBCC). (1995). Institute for Research in Construction, National Research Council Canada.
 Ohkuma, T., Marukawa, H., Yoshie, K., Niwa, H., Teramoto, T., and Kitamura, H. (1995). "Simulation method of simultaneous time-series of multi-local wind forces on tall buildings by using dynamic balance data." *J. Wind. Eng. Ind. Aerodyn.*, 54/55, 115–123.
 Reinhold, T. A., and Kareem, A. (1986). "Wind loads and building response predictions using force balance techniques." *Proc., 3rd ASCE Engineering Mechanics Conf.—Dynamics of Structures*, UCLA, Los Angeles.
 Repetto, M. P., and Solari, G. (2004). "Equivalent static wind actions on vertical structures." *J. Wind. Eng. Ind. Aerodyn.*, 92(5), 335–357.
 Shimada, K., Tamura, Y., Fujii, K., and Wakahara, T. (1990). "Wind induced torsional motion of tall building." *Proc., 11th National Symp. on Wind Engineering*, Tokyo, 221–226 (in Japanese).
 Solari, G., and Pagnini, L. C. (1999). "Gust buffeting and aeroelastic

- behavior of poles and monotubular towers." *J. Fluids Struct.*, 13, 877–905.
- Solari, G., Reinhold, T. A., and Livesey, F. (1998). "Investigation of wind actions and effects on the leaning Tower of Pisa." *Wind Struct.*, 1(1), 1–23.
- Tallin, A., and Ellingwood, B. (1985). "Wind induced lateral-torsional motion of buildings." *J. Struct. Eng.*, 111(10), 2197–2213.
- Tamura, Y., Kawai, H., Uematsu, Y., Kondo, K., and Ohkuma, T. (2003a). "Revision of AIJ Recommendation for wind loads on buildings." *Proc., International Wind Engineering Symp., IWES*, Tamsui, Taipei County, Taiwan.
- Tamura, Y., Kikuchi, H., and Hibi, K. (2003b). "Quasi-static wind load combinations for low- and middle-rise buildings." *J. Wind. Eng. Ind. Aerodyn.*, 91(12–15), 1613–1625.
- Tschanz, T., and Davenport, A. G. (1983). "The base balance technique for the determination of dynamic wind loads." *J. Wind. Eng. Ind. Aerodyn.*, 13(1–3), 429–439.
- Vickery, B. J., and Basu, R. I. (1984). "The response of reinforced concrete chimneys to vortex shedding." *Eng. Struct.*, 6, 324–333.
- Vickery, P. J., Steckley, A. C., Isyumov, N., and Vickery, B. J. (1985). "The effect of mode shape on the wind induced response of tall buildings." *Proc., 5th United States National Conf. on Wind Engineering*, Texas Tech. Univ., Lubbock, Tex., 1B-41–1B-48.
- Xie, J., and Irwin, P. A. (1998). "Application of the force balance technique to a building complex." *J. Wind. Eng. Ind. Aerodyn.*, 77/78, 579–590.
- Xie, J., Kumar, S., and Gamble, S. (2003). "Wind loading study for tall buildings with similar dynamic properties in orthogonal directions." *Proc., 10th International Conf. on Wind Engineering*, Copenhagen, Denmark, 2389–2396.
- Xu, Y. L., and Kwok, K. C. S. (1993). "Mode shape corrections for wind tunnel tests of tall buildings." *Eng. Struct.*, 15, 618–635.
- Yip, D. Y. N., and Flay, R. G. J. (1995). "A new force balance data analysis method for wind response predictions of tall buildings." *J. Wind. Eng. Ind. Aerodyn.*, 54/55, 457–471.
- Zhou, Y., and Kareem, A. (2001). "Gust loading factor: New model." *J. Struct. Eng.*, 127(2), 168–175.
- Zhou, Y., Kareem, A., and Gu, M. (2002). "Mode shape corrections for wind load effects." *J. Eng. Mech.*, 128(1), 15–23.